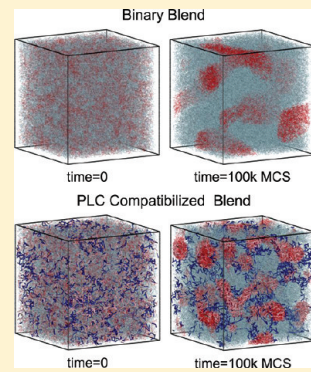


Phase Separation Dynamics for a Polymer Blend Compatibilized by Protein-like Copolymers: A Monte Carlo Simulation

Ravish Malik, Carol K. Hall, and Jan Genzer*

Department of Chemical & Biomolecular Engineering, North Carolina State University, Raleigh, North Carolina 27695-7905, United States

ABSTRACT: We use Monte Carlo simulation based on the bond fluctuation model to investigate how adding $\approx 4.92\%$ protein-like copolymer (PLC) to an immiscible binary polymer blend affects the dynamics of phase separation. PLCs slow down effectively the process of phase separation in binary blends by migrating to the biphasic interface between the immiscible homopolymers, thereby reducing the interfacial tension. The ability of PLCs to retard effectively the process of phase separation depends sensitively on the interaction energy between the PLCs and homopolymers and the PLC chain length. PLCs compatibilize the binary blend more effectively with increasing attractive interaction between the PLC blocks and homopolymers. Nominal improvement in compatibilization of the binary blend is achieved with increasing PLC chain length. The growth of phase-separated domains follows a dynamical scaling law for both the binary blend and PLC compatibilized ternary blend in the late stages of phase separation. The universal scaling functions are nearly independent of the interaction energy and PLC chain length. Thus, the phase-separated domains grow with dynamical self-similarity irrespective of the type of PLC added to the binary blend, although the type of PLC significantly alters the growth rate of the phase-separated domains.



INTRODUCTION

Macrophase separation in polymer blends limits their applicability as adhesives, interfacial stabilizers, coatings, membranes, ion-exchange systems, and functional materials for biomedical applications.¹ To arrest the process of phase separation in immiscible polymer blends, macromolecular compatibilizers are typically added. They localize at the interface between the immiscible homopolymers, thereby reducing interfacial tension and slowing down the process of phase separation, leading to finer domain dispersion and improved mechanical strength of the interface. Our recent computer simulation results suggest that protein-like copolymers (PLCs) could be used effectively as compatibilizers for immiscible homopolymer blends and might represent an attractive alternative to block, random, and alternating copolymer compatibilizers from a thermodynamic point of view.² In this study we investigate the dynamics of phase separation of an immiscible polymer blend in the presence of PLCs as compatibilizers.

Protein-like copolymers represent a new class of functional copolymers that exhibit large-scale compositional heterogeneities and long-range correlations along the comonomer sequence.³ The concept of PLCs was first introduced by Khokhlov and co-workers,^{3–5} who used computer simulations to demonstrate that random copolymers with tunable monomer sequence distributions could be generated by adjusting the compactness of a parent homopolymer composed of component A, and then converting exposed segments on the polymer coil surface into B segments by reacting them with other species in the surrounding solution.

In order to control the morphology and properties of immiscible polymer blends, it is necessary to understand the mechanisms

that govern the phase separation dynamics. These have been explored extensively both theoretically^{6–13} and experimentally.^{12,14–25} Particular attention has been paid to the impact of diblock compatibilizers on phase separation dynamics in immiscible polymer blends.^{26–34} Diblock copolymers are popular as compatibilizers due to their effectiveness in reducing the interfacial tension and increasing the mechanical strength of immiscible interfaces; these are affected in part by having the copolymer blocks entangle within the respective homopolymers. However, since diblock copolymers themselves microphase separate easily at higher copolymer loading,^{35–38} other copolymer sequences have been considered.^{34,39,40} This possibility has stimulated experimental and theoretical research on the dynamics of phase separation of immiscible homopolymers blends in the presence of random, alternating, random-blocky, random-alternating, and gradient copolymers^{41–45} as possible interfacial compatibilizers.

The dynamics of phase separation of immiscible homopolymer blends in the presence of PLCs as compatibilizers has not yet been explored. In this work, we use Monte Carlo (MC) simulation to investigate how adding protein-like copolymer (PLC) to an immiscible binary blend of homopolymers affects the phase separation dynamics. The effects of the pairwise interaction parameters between the homopolymers and the PLC blocks (which may be chemically different) and the effects of variation in the PLC chain length on the phase separation dynamics in immiscible blends are examined.

Received: June 29, 2011

Revised: September 1, 2011

Published: September 22, 2011

MC simulations based on the bond fluctuation model are performed on an immiscible binary blend containing 9736 20-mers of homopolymer A and 2434 20-mers of homopolymer B, to which $\approx 4.92\%$ PLCs containing equal numbers of C and D monomers is added. Both the binary blend (A/B) and ternary blend (A/B/C-plc-D) are mixed uniformly in the initial state. Phase separation between homopolymers A and B is induced by introducing positive pairwise interactions between monomer A and B units. As the immiscible polymer blend phase-separates, A-rich and B-rich homopolymer domains start to form and grow. This process is retarded in the compatibilized blend as the PLCs localize to the biphasic interface between the two homopolymers minimizing the unfavorable interactions and reducing the interfacial tension. The process of phase separation is monitored by recording the number of contacts between segments of A–A ($\langle n_{AA}(t) \rangle$), B–B ($\langle n_{BB}(t) \rangle$), and A–B ($\langle n_{AB}(t) \rangle$). The extent of penetration of PLCs into the homopolymer-rich phase over time is monitored by recording the fraction of contacts made by the PLC segments with homopolymer segments $f_{CA}(t)$, $f_{CB}(t)$, $f_{DA}(t)$, and $f_{DB}(t)$. The extent of PLC chain expansion with time is recorded by evaluating the normalized radius of gyration $\langle R_g^2(t) \rangle / \langle R_g^2(0) \rangle$ of the PLC. The dynamics of phase separation in both the binary and the ternary blend is measured using the time-dependent collective structure factor $S(q,t)$. To gauge the compatibilization effectiveness of various PLC types (as characterized by PLC–homopolymer interaction strength parameters and the PLC chain length), the dynamic scaling exponent associated with $q_1(t)$, the first moment of the structure factor at time t , is calculated for the late stages of phase separation. To demonstrate the existence of self-similarity among the phase-separated structures developed at various times during the late stages of phase separation in both the binary and ternary blends, the structure factor $S(q,t)$ is scaled in terms of a characteristic length parameter $1/q_1(t)$ and scaling function $F(x)$, and the time invariance of $F(x)$ is tested in the late stages of phase separation. The universality of the scaling function is verified for various types of ternary blends compatibilized by PLCs.

Highlights of our results are as follows. C-plc-D copolymers compatibilize effectively the blend by migrating to the biphasic interface between the immiscible homopolymers, thereby reducing the unfavorable interactions between the immiscible homopolymers. The ability of PLCs to retard effectively the process of phase separation depends sensitively on the interaction energy between the PLCs and homopolymers and the PLC chain length. PLCs compatibilize the A/B blend more effectively as the attractive interaction between the PLC C (or D) segments and homopolymers A (or B) increases. Marginal improvement in compatibilization of the A/B blend is achieved with increasing PLC chain length. The phase-separated structures developed at various times during the late stages of phase separation exhibit self-similarity in both the binary and ternary blends; i.e., the morphology change with time involves only an increase in the size of phase-separated domains and not any change in the interfacial structure. As a consequence, the late stage structure factor $S(q,t)$ can be rewritten in terms of a characteristic length parameter $1/q_1(t)$ and a time-invariant scaling function $F(x)$. $F(x)$ is universal as it is nearly independent of the PLC–homopolymer interaction strength parameters, and the PLC chain length for PLC compatibilized ternary blends during the late stages of phase separation.

In the next section, we describe the MC method and the generation of PLCs via the instant coloring procedure of

Table 1. Matrix of Interaction Parameters

		ε_{ij}		
		A	B	C
				D
A	0	0.5	varied to be -0.1 , -0.2 , -0.5	0.5
B		0	0.5	varied to be -0.1 , -0.2 , -0.5
C			0	0.5
D				0

Khokhlov and co-workers. The following section presents the simulation results for dynamics of phase separation of immiscible binary blends in the presence of PLC sequences. The final section concludes with a short summary of the results and a discussion.

■ MODEL AND METHOD

The A/B binary blend system consists of 9736 20-mers of type A and 2434 20-mers of type B. The ternary (compatibilized) system comprises the binary blend plus protein-like copolymer chains ($\approx 4.92\%$ of total number of segments in the ternary blend system) containing monomers of types C and D having compositions $x_C = x_D = 0.5$. The PLCs and homopolymers are modeled as self-avoiding walks on a three-dimensional bond-fluctuation cubic lattice. The chain length of the PLC compatibilizer is varied to be 30, 50, and 70 segments, while the amount of PLCs added to the binary blend is held fixed. The phase separation of homopolymer chains A and B is induced by introducing positive repulsive pairwise interaction energy between A and B segments $\varepsilon_{AB} = \varepsilon_{AB}'/k_B T = 0.5$ in both the binary and ternary blend systems. Since the symmetric C–D PLC compatibilizer is composed of segments that are chemically different from the homopolymer units, one must specify 10 monomer–monomer interaction parameters: ε_{AB} , ε_{AC} , ε_{AD} , ε_{BC} , ε_{BD} , ε_{CD} , ε_{AA} , ε_{BB} , ε_{CC} , and ε_{DD} . The values of ε are listed in Table 1. The interaction energies between the segments of homopolymer A and the segments of type C (ε_{AC}) on the C–D PLC and between the segments of homopolymer B and the segments of type D (ε_{BD}) on the C–D PLC are both chosen to be negative, so that C–D PLCs become effective compatibilizing agents for the immiscible A/B binary blend. The strengths of the interaction energies $\varepsilon_{AC} = \varepsilon_{BD}$ are varied to be -0.1 , -0.2 , and -0.5 . The interaction energies ε_{AD} , ε_{BC} , and ε_{CD} are all set equal to 0.5 to discourage miscibility between their corresponding segments. The interaction energies between identical segments are set to zero ($\varepsilon_{AA} = \varepsilon_{BB} = \varepsilon_{CC} = \varepsilon_{DD} = 0$). Additionally, the interaction energies between each segment type and the empty sites are set to zero.

The lattice MC simulations are based on the three-dimensional bond fluctuation model (BFM)⁴⁶ performed in the NVT ensemble. We chose the BFM to model the dynamics of phase separation in polymer blends since it has been utilized previously^{47–50} to predict the properties of dense polymer melts successfully. The BFM possesses some of the flexibility associated with an off-lattice model while maintaining the advantages associated with working on a lattice, such as integer arithmetic and parallelization.⁵¹ The lattice MC simulations are performed on a simple cubic lattice of $L \times L \times L$ sites with $L = 80$. The volume fraction, $\phi = N/L^3$, for the pure as well as compatibilized blend is set to $\phi = 0.5$, where N is the number of occupied sites in

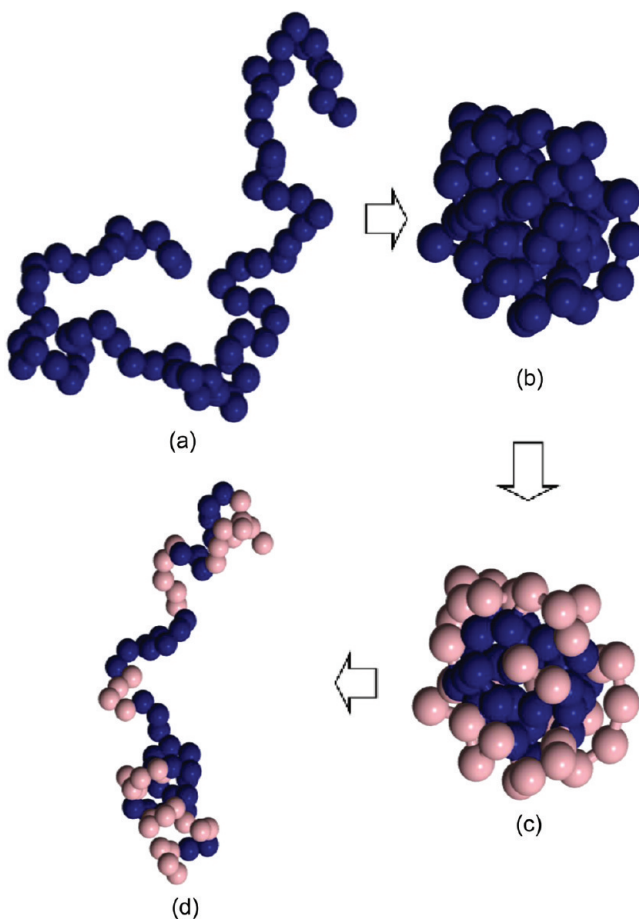


Figure 1. Snapshots illustrating instantaneous coloring procedure to generate 70-mer CD PLC (C = dark blue, D = light pink) with composition $x_C = x_D = 0.5$: (a) random configuration of 70-mer C chain, (b) collapsed globular configuration of the C chain, (c) 35 spheres farthest from the center of the globule are colored to type D, and (d) relaxed chain configuration of the resulting CD 70-mer PLC.

the simulation box. Periodic boundary conditions are imposed in all three directions (x , y , and z) to overcome the limitation of finite system size.

The symmetric C–D PLCs were generated via a simulation-based instantaneous coloring procedure originally proposed by Khokhlov et al.^{3–5} A detailed description of our implementation of Khokhlov's coloring procedure to generate C–D PLCs (with chain lengths 30, 50, and 70) via discontinuous molecular dynamics (DMD) simulation can be found in our previous work.² To prepare the symmetric C–D 70-mer PLC, a 70-mer C chain with square well interactions between nonadjacent C monomer segments was initialized in a random coil configuration. Figure 1a shows a snapshot of a sample initial configuration. Discontinuous molecular dynamics simulations² were performed on the C chain at a low reduced temperature until the C chain collapsed to a globular conformation as shown in Figure 1b. The segments in the final globular conformation were sorted in order of their distance from the center of the globule. The 35 segments of type C farthest from the center were colored to be D as depicted in Figure 1c. The coloring procedure resulted in the creation of a 70-mer C–D PLC with a composition of $x_C = x_D = 0.5$. After the coloring procedure, the configuration of the C–D PLC was relaxed. Figure 1d shows a snapshot of a sample

C–D 70-mer PLC generated via the instantaneous coloring procedure.

MC simulations were performed on the binary and ternary blend systems. The simulations on the blend systems were started in a random configuration at the desired volume fraction. Initially the blend systems were uniformly mixed, but once the interactions were turned on MC simulations were performed for 100 000 Monte Carlo steps (MCS); the systems demix sufficiently into homopolymer A-rich and homopolymer B-rich phase for us to consider this a phase-separated system. In each MCS, all beads in the system are moved once on average.

To monitor the dynamics of phase separation, the following measures are used: (1) the normalized number of nearest-neighbor contacts between segments of A–A ($\langle n_{AA}(t) \rangle / \langle n_{AA}(0) \rangle$), B–B ($\langle n_{BB}(t) \rangle / \langle n_{BB}(0) \rangle$), and A–B ($\langle n_{AB}(t) \rangle / \langle n_{AA}(0) \rangle$) where t is the time elapsed since the start of the phase separation, (2) the fraction of the nearest-neighbor contacts between the PLC and homopolymer segments $f_{CA}(t)$, $f_{CB}(t)$, $f_{DA}(t)$, and $f_{DB}(t)$, (3) the PLC chain expansion ratio, i.e., the normalized PLC radius of gyration $\langle R_g^2(t) \rangle / \langle R_g^2(0) \rangle$, (4) the time-dependent collective structure factor for the binary blend and the ternary compatibilized blends, (5) the first moment of the structure factor vs time, (6) the scaling exponent, which is obtained from the slope of the first moment of the structure factor vs time during the later stage of phase separation, and (7) the scaling function during the late stages of phase separation.

The fraction of contacts made by the C segments of the C–D PLC with homopolymer segments A, $f_{CA}(t)$, is defined by the following equation:

$$f_{CA}(t) = \langle n_{CA}(t) / (n_{CA}(t) + n_{CB}(t)) \rangle \quad (1)$$

where $n_{CA}(t)$ and $n_{CB}(t)$ refer to the nearest-neighbor contacts between segments of C–A and C–B, respectively, at time t . Similarly, $f_{CB}(t)$, $f_{DA}(t)$, and $f_{DB}(t)$ can also be defined.

The PLC chain expansion ratio is $\langle R_g^2(t) \rangle / \langle R_g^2(0) \rangle$, where $\langle R_g^2(t) \rangle$ is defined by the following equation

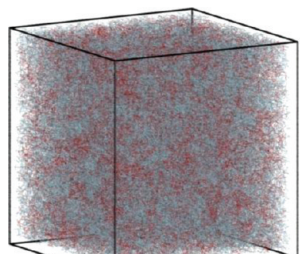
$$\langle R_g^2(t) \rangle = \sum_{i=1}^{N_{PLC}} \sum_{j=1}^{n_{segment}} \{r_{i,j}(t) - r_i^{cm}(t)\}^2 / \{N_{PLC} n_{segment}\} \quad (2)$$

In eq 2, $\langle R_g^2(t) \rangle$ is the PLC radius of gyration at time t while $\langle R_g^2(0) \rangle$ is the PLC radius of gyration initially, $r_{i,j}(t)$ is the position of the j th monomer on the i th PLC chain at time t and $r_i^{cm}(t)$ is the position of the center of mass of the i th PLC chain at time t , N_{PLC} is the number of PLC chains, and $n_{segment}$ is the number of spheres in a single PLC chain.

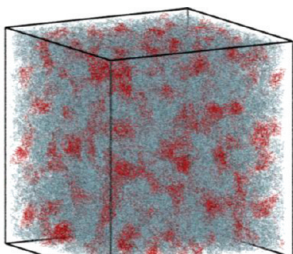
The time-dependent collective structure factor for both the binary and ternary blend systems⁵² is evaluated to monitor the time evolution of the long-range ordering. The structure factor is the Fourier transform of the pair correlation function and is defined by the following equation:

$$S(q, t) = \langle [\sum_j (\exp(i\mathbf{q} \cdot \mathbf{r}_j)) (\phi_A^j(t) - \langle \phi_A^j \rangle)(\phi_B^j(t) - \langle \phi_B^j \rangle)]^2 \rangle / L^3 \quad (3)$$

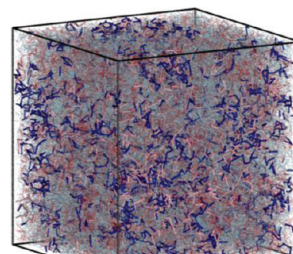
where L is the box length, the scattering vector \mathbf{q} is defined as $\mathbf{q} = 2\pi\mathbf{n}/L$, where \mathbf{n} represents a positive integer vector, i.e. $\mathbf{n} = (n_x, n_y, n_z)$, the local concentration variable $\phi_A^j(t)$ (or $\phi_B^j(t)$) at time t is equal to one if lattice site j is occupied by an A (or B) segment and zero otherwise, and the outer angular brackets $\langle \dots \rangle$



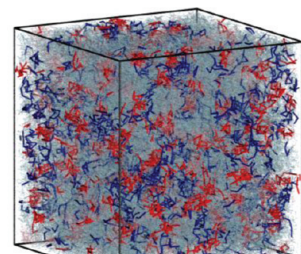
(a)



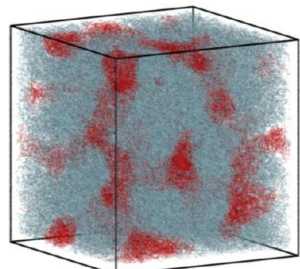
(b)



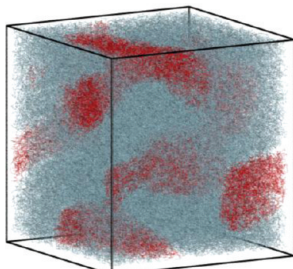
(a)



(b)



(c)



(d)

Figure 2. Simulation snapshots of the A/B binary blend (A = light blue, B = red) at time (a) $t = 0$ (initial configuration), (b) $t = 5\text{k MCS}$ (early stage configuration), (c) $t = 50\text{k MCS}$ (halfway configuration), and (d) $t = 100\text{k MCS}$ (final configuration).

denote a thermal statistical average. The contribution from the PLC chains to the collective structure factor is neglected since we are principally interested in the phase separation of homopolymers A and B, and the PLC compatibilizer loading ($\approx 4.92\%$) is small relative to the homopolymers. To improve the statistics in q space, the collective structure factor is spherically averaged as follows:

$$S(q, t) = \sum_{q - (\Delta q/2) \leq q \leq q + (\Delta q/2)} S(q, t) / m(q, \Delta q) \quad (4)$$

where

$$m(q, \Delta q) = \sum_{q - (\Delta q/2) \leq q \leq q + (\Delta q/2)} 1 \quad (5)$$

denotes the number of lattice points in a spherical shell of radius q with Δq as the shell thickness. In scattering experiments (using x-rays, neutrons, or light) on real immiscible polymer blends the intensity of radiation scattered or the structure factor $S(q, t)$ is small initially (for all values of the scattering vector or scattering angle q) as the homopolymers are uniformly mixed, but a distinct peak in the structure factor $S(q^*, t)$ develops at a scattering vector q^* as the phase separation occurs. Physically at time t , $1/q^*$ is a measure of the characteristic length scale in the blend while $S(q^*, t)$ is a measure of the difference in concentrations of the constituent homopolymers in the polymer blend.

We evaluate the first moment $q_1(t)$ of the structure factor $q_1(t) = \sum_q S(q, t) / \sum_q S(q, t)$. The inverse of $q_1(t)$ is a measure of the average domain size of the phase-separated domains in both the binary and ternary blends. It is well-known that $q_1(t)$ is time invariant in the early stage of phase separation where Cahn's linearized theory^{6,53} is applicable. In the late stages $q_1(t)$ decreases with increasing phase separation time due to growth in the size of the phase-separated domains. The time

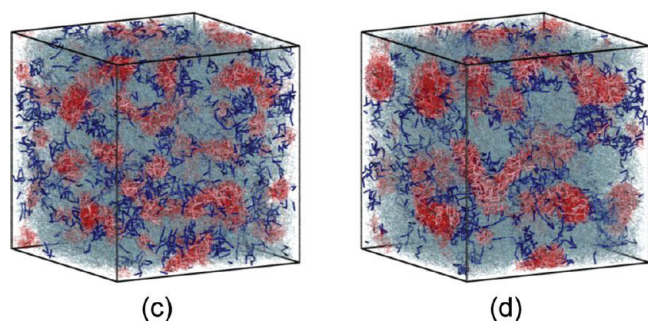


Figure 3. Simulation snapshots of the A/B/C-plc-D ternary blend (A = light blue, B = red, C = dark blue, D = light pink) compatibilized by 70-mer PLC with $\varepsilon_{AC} = \varepsilon_{BD} = -0.5$ at time (a) $t = 0$ (initial configuration), (b) $t = 5\text{k MCS}$ (early stage configuration), (c) $t = 50\text{k MCS}$ (intermediate configuration), and (d) $t = 100\text{k MCS}$ (final configuration).

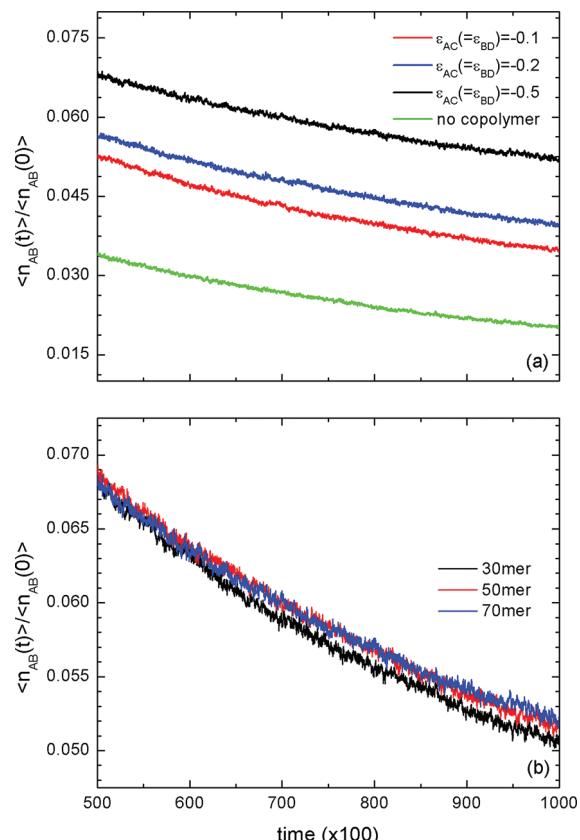


Figure 4. Normalized A–B contacts $\langle n_{AB}(t) \rangle / \langle n_{AB}(0) \rangle$ with phase separation time: (a) interaction energy ε_{AC} varied (70-mer PLC) and (b) PLC chain length varied (fixed interaction energy $\varepsilon_{AC} = \varepsilon_{BD} = -0.5$).

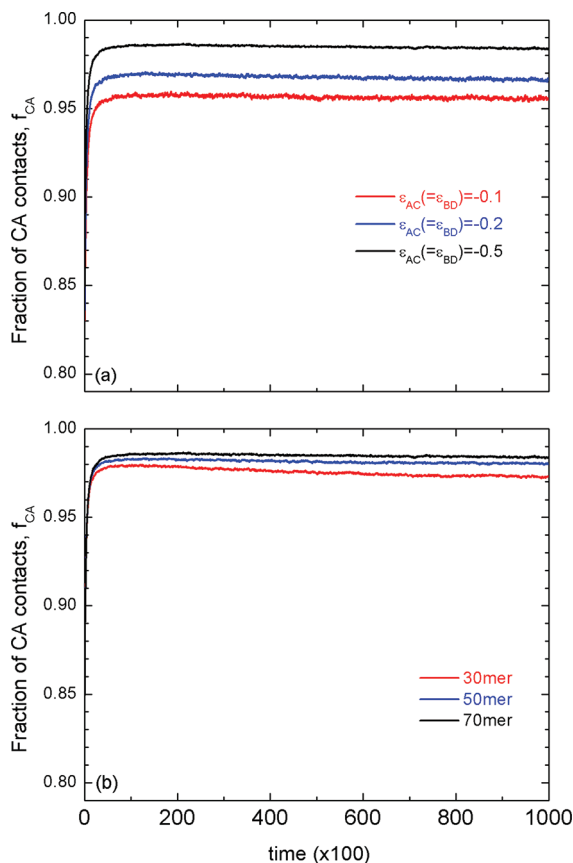


Figure 5. Fraction of C–A contacts $f_{CA}(t)$ with phase separation time: (a) interaction energy ε_{AC} varied (70-mer PLC) and (b) PLC chain length varied (fixed interaction energy $\varepsilon_{AC} = \varepsilon_{BD} = -0.5$).

dependence of $q_1(t)$ in the later stage of phase separation is characterized by the following power law⁹ equation:

$$q_1(t) \sim t^{-n} \quad (6)$$

where n is the scaling or dynamical exponent whose value depends on the mechanism of domain growth. Although the scaling exponent is generally a function of phase separation time and temperature, it tends to reach $1/3$ for $t \rightarrow \infty$ when long-range hydrodynamic interactions are absent,⁵⁴ which is the case in our simulation. When long-range hydrodynamic interactions are significant,^{55,56} $n = 1$. We obtain the scaling exponent from the slope of the log–log plot of $q_1(t)$ versus time in the late stages of phase separation for both the binary and ternary blends. The scaling exponent is useful for comparing the compatibilization effectiveness of various types of PLCs based on the values of the interaction energies and chain length. The smaller the value of the scaling exponent in a PLC compatibilized blend, the more effective the PLC acts as a compatibilizer. A smaller value of the scaling exponent implies a higher value of the slope in the log–log plot of $q_1(t)$ versus time during the late stages of phase separation, which, in turn, implies a higher value of $q_1(t)$ or smaller domain size (since scattering vector and length scale are inversely related) of phase-separated structures and hence slower phase separation.

Phase-separated structures developed at various times during the late stages of phase separation in binary polymer blends exhibit self-similarity,^{24,57} i.e., the morphology change with time

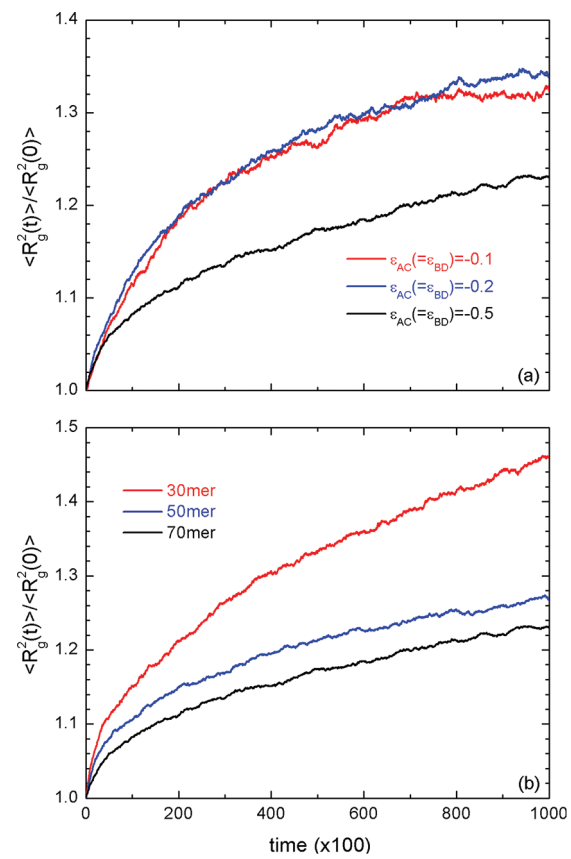


Figure 6. PLC chain expansion ratio or normalized radius of gyration $\langle R_g^2(t) \rangle / \langle R_g^2(0) \rangle$ with phase separation time: (a) interaction energy ε_{AC} varied (70-mer PLC) and (b) PLC chain length varied (fixed interaction energy $\varepsilon_{AC} = \varepsilon_{BD} = -0.5$).

involves only an increase in the size of the phase-separated domains but not a change in the interfacial structure. If self-similarity exists between the phase-separated structures developed at various times during the late stages of phase separation for a demixing polymer blend, the structure factor can be rewritten in terms of a single time-dependent length parameter $1/q_1(t)$ and the scaling function $F(x)$ as described by the following equation

$$S(q, t) = [1/q_1(t)]^3 F(x)/G \quad (7)$$

where $x = q/q_1(t)$ is the reduced scattering vector, $F(x)$ is the scaling function, and G is an arbitrary normalization constant. If the scaling law as described by eq 7 holds for the binary polymer blend during the late stages of phase separation, the scaling function $F(x)$ becomes independent of time during the late stages of phase separation. The scaling law for immiscible binary blends described above has also been shown to hold for binary blends compatibilized by diblock copolymers in the late stage of phase separation^{29–31} with the normalization constant $G = (\pi \sum_q q^2 S(q, t))^{-1} L$, where L is the length of the simulation box. We test the validity of the scaling law as described in eq 7 for binary blends compatibilized by PLCs.

The properties for both the binary and ternary blend systems were averaged over five runs starting from uncorrelated random initial configurations. The results for ternary blends compatibilized by PLCs were averaged over three different copolymer sequences for a given initial configuration (five different initial

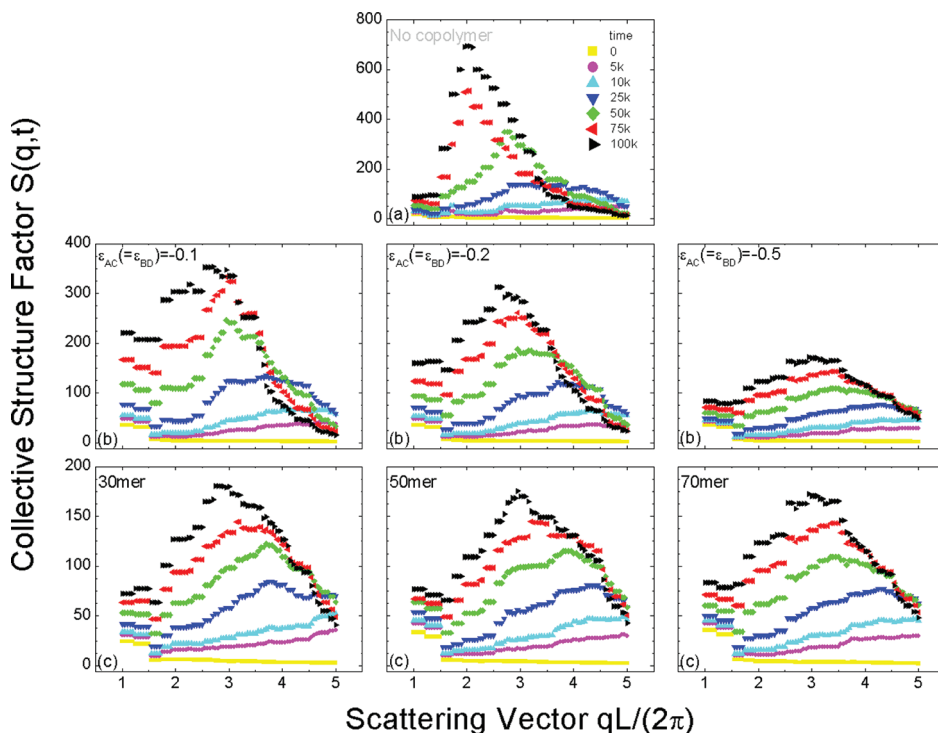


Figure 7. Evolution of $S(q,t)$ with phase separation time for (a) binary A/B blend; (b) ternary A/B/C-plc-D blend, interaction energy ε_{AC} varied (70-mer PLC); and (c) ternary A/B/C-plc-D blend, PLC chain length varied (fixed interaction energy $\varepsilon_{AC} = \varepsilon_{BD} = -0.5$).

configurations) and set of interaction energy parameters ($\varepsilon_{AC} = -0.1$, $\varepsilon_{AC} = -0.2$, and $\varepsilon_{AC} = -0.5$) and chain lengths (30-, 50-, and 70-mers). Thus, 135 simulations were performed for ternary blends compatibilized by PLCs. The errors which represent the sample standard deviations of the properties calculated were within 5%. We chose not to display the errors bars, which are relatively small, on the plots for the sake of clarity.

RESULTS AND DISCUSSION

Snapshots of the asymmetric binary blend system are shown in Figure 2 at various times during the demixing process. Figure 2 shows the binary blend (a) initially, (b) at a very early stage in the simulation (5k MCS), (c) halfway through the simulation (50k MCS), and (d) at the end of the simulation (100k MCS). As the phase separation progresses, homopolymer A-rich and homopolymer B-rich domains begin to form and grow. Figure 3 shows the ternary PLC compatibilized blend (a) initially, (b) at a very early stage in the simulation (5k MCS), (c) halfway through the simulation (50k MCS), and (d) at the end of the simulation (100k MCS). Comparison of Figures 2 and 3 gives a sense of how the presence of PLC compatibilizer retards the phase separation of the binary blend. In the ternary blend, homopolymer A-rich and homopolymer B-rich domains form and grow as was the case for the binary blend, but this time the PLCs migrate to the biphasic interface between the two homopolymers, reducing unfavorable contacts, minimizing interfacial energy, and binding the two homopolymer phases together.

The process of phase separation in both binary and ternary blends is accompanied by a change in the number of A–A, B–B, and A–B contacts with time. We expect the number of A–A and B–B contacts to increase and the number of A–B contacts to

decrease with phase separation time. Figure 4 shows a plot of the normalized number of A–B contacts $\langle n_{AB}(t)/n_{AB}(0) \rangle$ with phase separation time. The time has been restricted to the latter half of the simulation for clarity. In Figure 4a, the PLC chain length is fixed to be 70 while the interaction energy is varied. As the strength of the favorable interaction energy between the PLC blocks and homopolymers increases, the normalized number of A–B contacts increases, implying an increase in the effectiveness of PLCs as compatibilizers. In Figure 4b the interaction energy is fixed to be $\varepsilon_{AC} = \varepsilon_{BD} = -0.5$ while the PLC chain length is varied. As the PLC chain is increased from 30 to 70, the normalized number of A–B contacts increases marginally, implying a nominal improvement in compatibilization effectiveness with increasing PLC chain length.

As the phase separation evolves in blends compatibilized by PLCs, the PLCs migrate to the biphasic interface between the two homopolymers to penetrate both homopolymer-rich phases. To monitor the extent of penetration of PLCs into the homopolymer-rich phases, we monitor the fraction of the contacts between the PLC and homopolymer segments $f_{CA}(t)$, $f_{CB}(t)$, $f_{DA}(t)$, and $f_{DB}(t)$. Since the interaction between components C and A is favorable, we expect $f_{CA}(t)$ to increase with time. Figure 5 shows a plot of the $f_{CA}(t)$ with phase separation time. In Figure 5a the PLC chain length is fixed to be 70 while the interaction energy is varied. As the strength of the favorable interaction energy between the PLC blocks and homopolymers increases, $f_{CA}(t)$ increases, implying the increase in effectiveness of PLCs as compatibilizers. In Figure 5b the interaction energy is fixed to be $\varepsilon_{AC} = \varepsilon_{BD} = -0.5$ while the PLC chain length is varied. As the PLC chain length is increased from 30 to 70, $f_{CA}(t)$ increases marginally, implying a nominal improvement in compatibilization effectiveness with increasing PLC chain length.

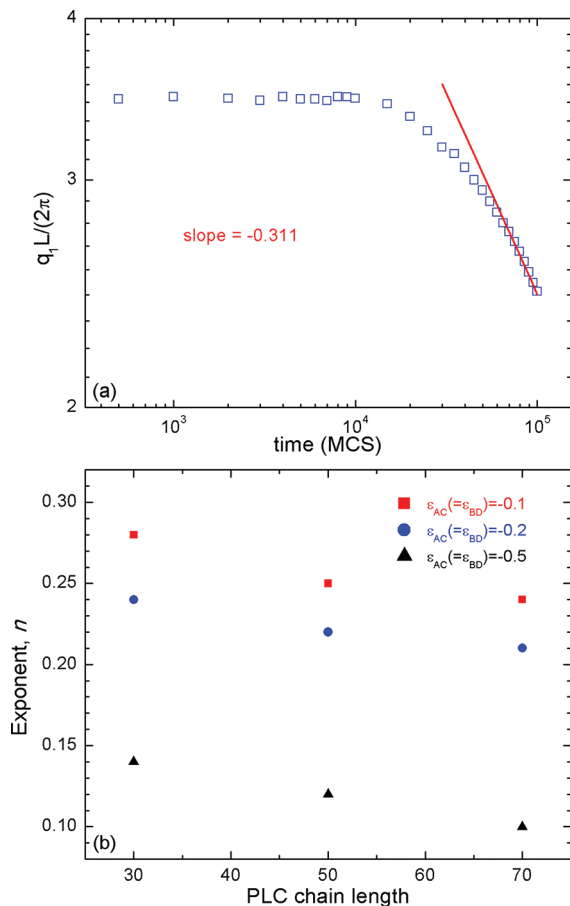


Figure 8. (a) $q_1(t)$ with phase separation time for A/B binary blend and (b) scaling exponent for the ternary A/B/C-plc-D blend.

Figure 6 depicts the PLC chain expansion ratio or normalized radius of gyration with phase separation time. In Figure 6a the PLC chain length is fixed to be 70 while the interaction energy is varied. In Figure 6b the interaction energy is fixed to be $\varepsilon_{AC} = \varepsilon_{BD} = -0.5$ while the PLC chain length is varied. The performance of PLCs as compatibilizers improves with increasingly favorable interaction energies between the PLC blocks and homopolymers and with PLC chain length. One would expect the effective PLC compatibilizers to have a higher PLC chain expansion ratio as they are likely to stretch more, forming engagements with the homopolymer-rich phases in comparison to ineffective PLC compatibilizers. However, we do not observe this trend here. We do not have a good explanation for this anomaly; it will be the subject of further investigation.

To quantify the extent of phase separation in both the binary and ternary compatibilized blends, we determine the spherically averaged time-dependent collective structure factor $S(q,t)$. Figure 7 shows a plot of $S(q,t)$ versus the scattering vector for both the binary and PLC compatibilized ternary blends. Initially as the blend is homogeneous $S(q,t)$ is small for all cases. With increasing phase separation time a distinct peak develops and the location of the peak shifts toward smaller values of the scattering vector, signifying the growth in size of the phase-separated domains. This behavior is also observed in scattering experiments on real polymer blends.^{11,15,17–22,24,57,58} An efficient compatibilizer would suppress the peak of $S(q,t)$ and shift it to higher values of the scattering vector. The structure factor for the binary blend

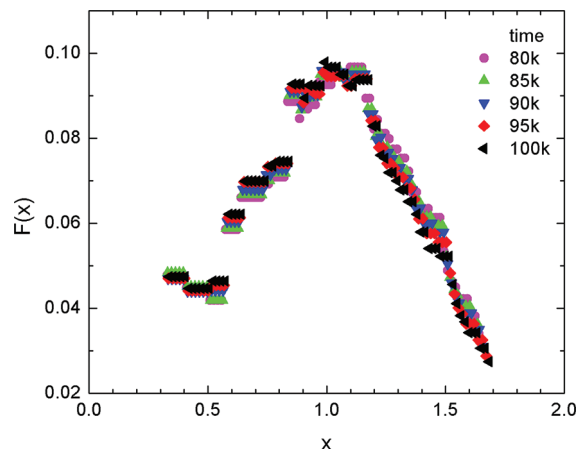


Figure 9. Scaling function in the late stage of phase separation for a binary blend compatibilized by 70-mer PLC with interaction energy $\varepsilon_{AC} = \varepsilon_{BD} = -0.5$.

without any PLC compatibilizer is shown in Figure 7a. In Figure 7b the PLC chain length is fixed to be 70 while the interaction energy is varied. As the strength of the favorable interaction energy between the PLC blocks and homopolymers increases, the peak in $S(q,t)$ is suppressed, implying an increase in effectiveness of PLCs as compatibilizers. In Figure 7c the interaction energy is fixed to be $\varepsilon_{AC} = \varepsilon_{BD} = -0.5$ while the PLC chain length is varied. As the PLC chain is increased from 30 to 70, the peak of $S(q,t)$ is suppressed marginally, implying a nominal improvement in compatibilization effectiveness with increasing PLC chain length.

To gain further insight into the time evolution of the structure factor in the late stage of phase separation, we evaluate the first moment of the structure factor $q_1(t)$. The inverse of $q_1(t)$ is a measure of the average size of the phase-separated domains in both the binary and ternary compatibilized blends. Figure 8a shows a log–log plot of $q_1(t)$ versus time for the binary polymer blend. In the early stage of phase separation $q_1(t)$ is time invariant, as predicted by Cahn's linearized theory.^{6,53} In the late stages of phase separation, $q_1(t)$ decreases with time due to growth in the size of the phase-separated domains. Since $q_1(t)$ in the late stage of phase separation can be characterized by a power law,⁹ we obtain the scaling exponent $n = 0.311$ from the slope of the plot in the late stage of phase separation. Our value is reasonably close to the theoretically accepted value of $n = 1/3$ for a binary blend under the asymptotic limit ($t \rightarrow \infty$) when long-range hydrodynamic interactions are insignificant,⁵⁴ which is the case in our simulation. In Figure 8b we plot the scaling exponent for the ternary blend compatibilized by PLCs of different chain lengths and interaction energies. The scaling exponent values shown are evaluated over roughly identical time intervals in order to make fair comparison between the phase separation processes. The smaller the value of the dynamic scaling exponent, the more effective the PLC is as a compatibilizer for the immiscible binary blend. A smaller value of the scaling exponent implies a higher value of the slope in the log–log plot of $q_1(t)$ versus time during the late stages of phase separation, which implies a higher value of $q_1(t)$ or smaller domain size (since scattering vector and length scale are inversely related) of phase-separated structures and hence slower phase separation. The scaling exponent analysis gives us a quick way to compare all of the nine ternary blend systems (3 PLC chain

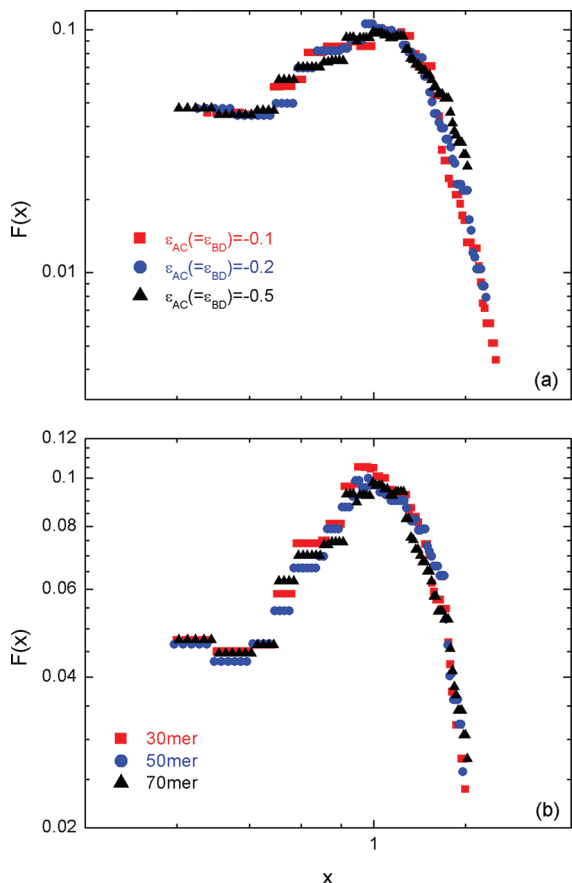


Figure 10. Scaling function in the late stages of phase separation for ternary A/B/C-plc-D blend: (a) interaction energy ε_{AC} varied (70-mer PLC) and (b) PLC chain length varied (fixed interaction energy $\varepsilon_{AC} = \varepsilon_{BD} = -0.5$).

lengths and 3 values of the interaction energies)—unlike the other analyses that we presented before in which the PLC interaction energy is held fixed while the PLC chain is varied and vice versa. Longer PLC chains which exhibit strong interaction with homopolymers are most effective in slowing down the process of phase separation in immiscible binary blends as they lead to smaller values of the dynamical scaling exponent.

To test the applicability of dynamical scaling laws in the late stage of phase separation in binary polymer blends compatibilized by PLCs, we evaluate the scaled structure factor as described earlier in the model and method section. Figure 9 shows a plot of the scaled structure factor, $F(x) = G[q_1(t)]^3 S(q,t)$, versus the reduced scattering angle $x = q/q_1(t)$ at various times in the late stages ($t \geq 80k$ MCS) of phase separation for a binary blend compatibilized by 70-mer PLC with interaction energy $\varepsilon_{AC} = \varepsilon_{BD} = -0.5$. Since the scaled structure factors at various times in the late stages of phase separation all fall on a single master curve, this establishes the existence of dynamical self-similarity among the growing phase-separated structures in the blend compatibilized by PLCs. Figure 10 shows a plot of the scaled structure factor at the end of the simulation (100k MCS) for the ternary A/B/C-plc-D blend compatibilized by various types of PLCs at various values of the interaction energies between the PLC blocks and homopolymers and the PLC chain length. In Figure 10a, the PLC chain length is fixed to be 70 and the interaction energy is varied. In Figure 10b, the interaction energy

is fixed to be $\varepsilon_{AC} = \varepsilon_{BD} = -0.5$ while the PLC chain length is varied. It is evident from Figure 10a,b that the scaled structure factor is nearly independent of both the interaction energy $\varepsilon_{AC} = \varepsilon_{BD}$ as well as the PLC chain length for all values of the reduced scattering angle explored by the simulation. This behavior implies universality of the scaled structure factor which means that the phase-separated domains in the ternary compatibilized blend grow with dynamical self-similarity irrespective of the type of PLC added.

CONCLUSIONS

We have performed Monte Carlo simulations aimed at understanding the effect of adding $\approx 4.92\%$ protein-like copolymer (PLC) on the dynamics of phase separation of a polymer blend containing two immiscible homopolymers A and B, where the C-plc-D copolymer used consists of blocks chemically different from the homopolymers. The ability of PLCs to effectively retard the process of phase separation depends sensitively on the interaction energy between the PLCs and homopolymers and the PLC chain length.

We have evaluated the number of nearest-neighbor contacts, the time-dependent collective structure factor, the first moment of the structure factor, and the dynamical scaling exponent to monitor the process of phase separation and gauge the effectiveness of various types of PLCs as characterized by the PLC–homopolymer interaction strength parameters and the PLC chain length. The effectiveness of PLCs as compatibilizers improves with increasingly favorable interaction energies between the PLC segments and homopolymers and with the PLC chain length. There is a limit to the enhancement in performance of PLCs as compatibilizers attained as the PLC chain length increases. Contrary to our expectation, the effective PLC compatibilizers (long PLC chains with strong interactions with homopolymers) do not stretch as much as the less effective PLC compatibilizers (short PLC chains with weak interactions with homopolymers). We do not have an explanation for this anomaly, and this will be subject of future investigation.

The process of phase separation in binary polymer blends compatibilized by PLCs obeys scaling laws during the late stage which implies the existence of self-similarity between the phase-separated structures developed at various times; i.e., the morphology change with time involves only an increase in the size of the phase-separated domains and no change in the interfacial structure. To the best of our knowledge, no experiments have been performed on using PLCs as compatibilizers for immiscible polymer blends. Scattering experiments on the dynamics of phase separation in blends compatibilized by PLCs are needed to validate our findings. It is interesting to note that scaling laws which hold for blends compatibilized by diblock^{29–31} copolymers also hold for PLC compatibilized blends.

The scaling functions in PLC compatibilized blends are universal as they are nearly independent of the interaction energy and the PLC chain length. Thus, the phase-separated domains grow with dynamical self-similarity irrespective of the type of PLCs added to the binary blend, although the type of PLC significantly alters the growth rate of the phase-separated domains.

Our work has practical implications for optimizing the performance of PLCs as compatibilizers for immiscible blends with respect to the PLC chain length and attractive interactive interaction energy between the PLC blocks and homopolymers. Optimizing the performance of PLCs as compatibilizers with

respect to the composition of PLCs and the case of PLCs with repulsive interactions with homopolymers will be subject of future work.

ACKNOWLEDGMENT

This work was supported by the Director, Office of Energy Research, Office of Basic Sciences, Chemical Science Division of the U.S. Department of Energy, under Grant DE-FG05-91ER14181 awarded to C.K.H. J.G. thanks the National Science Foundation for financial support through Grants DMR-0353102 and OISE-0730243.

REFERENCES

- (1) Robeson, L. M. Applications of Polymer Blends - Emphasis on Recent Advances. *Polym. Eng. Sci.* **1984**, *24*, 587–597.
- (2) Malik, R.; Hall, C. K.; Genzer, J. Protein-Like Copolymers (PLCs) as Compatibilizers for Homopolymer Blends. *Macromolecules* **2010**, *43*, 5149–5157.
- (3) Khokhlov, A. R.; Khalatur, P. G. Conformation-dependent sequence design (engineering) of AB copolymers. *Phys. Rev. Lett.* **1999**, *82*, 3456–3459.
- (4) Khalatur, P. G.; Ivanov, V. A.; Shusharina, N. P.; Khokhlov, A. R. Protein-like copolymers: computer simulation. *Russ. Chem. B+* **1998**, *47*, 855–860.
- (5) Khokhlov, A. R.; Khalatur, P. G. Protein-like copolymers: Computer simulation. *Physica A* **1998**, *249*, 253–261.
- (6) Degennes, P. G. Dynamics of Fluctuations and Spinodal Decomposition in Polymer Blends. *J. Chem. Phys.* **1980**, *72*, 4756–4763.
- (7) Pincus, P. Dynamics of Fluctuations and Spinodal Decomposition in Polymer Blends 0.2. *J. Chem. Phys.* **1981**, *75*, 1996–2000.
- (8) Binder, K. Collective Diffusion, Nucleation, and Spinodal Decomposition in Polymer Mixtures. *J. Chem. Phys.* **1983**, *79*, 6387–6409.
- (9) Gunton, J. D.; San Miguel, M.; Sanhi, P.; Domb, C.; Lebowitz, J. L., Eds.; Academic Press: New York, 1983; Vol. 8, p 157.
- (10) Hashimoto, T.; Ottenbrite, R. M.; Utracki, L. A.; Inoue, T., Eds.; Hanser: Munich, 1984; Vol. 2, p 199.
- (11) Strobl, G. R. Structure Evolution During Spinodal Decomposition of Polymer Blends. *Macromolecules* **1985**, *18*, 558–563.
- (12) Nose, T. Kinetics of Phase-Separation in Polymer Mixtures. *Phase Transitions* **1987**, *8*, 245–260.
- (13) Chakrabarti, A.; Toral, R.; Gunton, J. D.; Muthukumar, M. Dynamics of Phase-Separation in a Binary Polymer Blend of Critical Composition. *J. Chem. Phys.* **1990**, *92*, 6899–6909.
- (14) Snyder, H. L.; Meakin, P.; Reich, S. Dynamical Aspects of Phase-Separation in Polymer Blends. *Macromolecules* **1983**, *16*, 757–762.
- (15) Hashimoto, T.; Kumaki, J.; Kawai, H. Time-Resolved Light-Scattering-Studies on Kinetics of Phase-Separation and Phase Dissolution of Polymer Blends 0.1. Kinetics of Phase-Separation of a Binary Mixture of Polystyrene and Polyvinyl Methyl-Ether). *Macromolecules* **1983**, *16*, 641–648.
- (16) Gelles, R.; Frank, C. W. Effect of Molecular-Weight on Polymer Blend Phase-Separation Kinetics. *Macromolecules* **1983**, *16*, 1448–1456.
- (17) Hashimoto, T.; Sasaki, K.; Kawai, H. Time-Resolved Light-Scattering Studies on The Kinetics of Phase-Separation and Phase Dissolution of Polymer Blends 0.2. Phase-Separation of Ternary Mixtures of Polymer-A, Polymer-B, and Solvent. *Macromolecules* **1984**, *17*, 2812–2818.
- (18) Hashimoto, T.; Itakura, M.; Hasegawa, H. Late Stage Spinodal Decomposition of a Binary Polymer Mixture 0.1. Critical Test of Dynamic Scaling on Scattering Function. *J. Chem. Phys.* **1986**, *85*, 6118–6128.
- (19) Hashimoto, T.; Itakura, M.; Shimizu, N. Late Stage Spinodal Decomposition of a Binary Polymer Mixture 0.2. Scaling Analyses on $Q_m(\tau)$ and $I_m(\tau)$. *J. Chem. Phys.* **1986**, *85*, 6773–6786.
- (20) Han, C. C.; et al. Static and Kinetic-Studies of Polystyrene Poly(Vinylmethylether) Blends. *Polym. Eng. Sci.* **1986**, *26*, 3–8.
- (21) Bates, F. S.; Wiltzius, P. Spinodal Decomposition of a Symmetric Critical Mixture of Deuterated and Protonated Polymer. *J. Chem. Phys.* **1989**, *91*, 3258–3274.
- (22) Takenaka, M.; Izumitani, T.; Hashimoto, T. Slow Spinodal Decomposition in Binary-Liquid Mixtures of Polymers 0.4. Scaled Structure Factor for Later Stage Unmixing. *J. Chem. Phys.* **1990**, *92*, 4566–4575.
- (23) Hashimoto, T.; Takenaka, M.; Izumitani, T. Spontaneous Pinning of Domain Growth during Spinodal Decomposition of Off-Critical Polymer Mixtures. *J. Chem. Phys.* **1992**, *97*, 679–689.
- (24) Takenaka, M.; Hashimoto, T. Scattering Studies of Self-Assembling Processes of Polymer Blends in Spinodal Decomposition 0.2. Temperature-Dependence. *J. Chem. Phys.* **1992**, *96*, 6177–6190.
- (25) Takenaka, M.; Izumitani, T.; Hashimoto, T. Spontaneous Pinning of Domain Growth during Spinodal Decomposition of Off-Critical Polymer Mixtures 0.2. Scaling Analysis. *J. Chem. Phys.* **1993**, *98*, 3528–3539.
- (26) Roe, R. J.; Kuo, C. M. Effect of Added Block Copolymer on Phase-Separation Kinetics of a Polymer Blend 0.1. A Light-Scattering Study. *Macromolecules* **1990**, *23*, 4635–4640.
- (27) Park, D. W.; Roe, R. J. Effect of Added Block Copolymer on the Phase-Separation Kinetics of a Polymer Blend 0.2. Optical Microscopic Observations. *Macromolecules* **1991**, *24*, 5324–5329.
- (28) Hashimoto, T.; Izumitani, T. Effect of a Block-Copolymer on the Kinetics of Spinodal Decomposition of Polymer Blends 0.1. Non-universality in Scaled Characteristic Quantities versus Reduced Time. *Macromolecules* **1993**, *26*, 3631–3638.
- (29) Izumitani, T.; Hashimoto, T. Effect of a Block-Copolymer on the Kinetics of Spinodal Decomposition of Polymer Blends 0.2. Scaled Structure Factor. *Macromolecules* **1994**, *27*, 1744–1750.
- (30) Jo, W. H.; Kim, S. H. Monte carlo simulation of the phase separation dynamics of polymer blends in the presence of block copolymers 0.1. Effect of the interaction energy and chain length of the block copolymers. *Macromolecules* **1996**, *29*, 7204–7211.
- (31) Kim, S. H.; Jo, W. H.; Kim, J. Monte Carlo simulation of phase separation dynamics of a polymer blend in the presence of block copolymer. Effect of block copolymer composition. *Macromolecules* **1996**, *29*, 6933–6940.
- (32) Kim, S. H.; Jo, W. H.; Kim, J. A. Monte Carlo simulation of phase separation dynamics of polymer blends in the presence of a block copolymer 0.3. Effect of interaction energies among constituent segments. *Macromolecules* **1997**, *30*, 3910–3915.
- (33) Kim, S. H.; Jo, W. H. Monte Carlo simulation of the phase separation dynamics of polymer blends in the presence of block copolymers. IV. Effects of chain length and composition of repulsive black copolymer. *J. Chem. Phys.* **1998**, *108*, 4267–4281.
- (34) Barham, B.; Fosser, K.; Voge, G.; Waldow, D.; Halasa, A. Phase separation kinetics of a polymer blend modified by random and block copolymer additives. *Macromolecules* **2001**, *34*, 514–521.
- (35) Leibler, L. Theory of Microphase Separation in Block Co-Polymers. *Macromolecules* **1980**, *13*, 1602–1617.
- (36) Tanaka, H.; Hashimoto, T. Stability Limits for Macro-Phase and Microphase Transitions and Compatibilizing Effects in Mixtures of A-B Block Polymers with Corresponding Homopolymers. *Polym. Commun.* **1988**, *29*, 212–216.
- (37) Shull, K. R.; Kramer, E. J.; Hadzioannou, G.; Tang, W. Segregation of Block Copolymers to Interfaces between Immiscible Homopolymers. *Macromolecules* **1990**, *23*, 4780–4787.
- (38) Shull, K. R.; Winey, K. I.; Thomas, E. L.; Kramer, E. J. Segregation of Block Copolymer Micelles to Surfaces and Interfaces. *Macromolecules* **1991**, *24*, 2748–2751.
- (39) Ko, M. J.; Kim, S. H.; Jo, W. H. The effects of copolymer architecture on phase separation dynamics of immiscible homopolymer blends in the presence of copolymer: a Monte Carlo simulation. *Polymer* **2000**, *41*, 6387–6394.
- (40) Kamath, S. Y.; Dadmun, M. D. The effect of chain architecture on the dynamics of copolymers in a homopolymer matrix: Lattice Monte

Carlo simulations using the bond-fluctuation model. *Macromol. Theory Simul.* **2005**, *14*, 519–527.

(41) Kim, J.; Gray, M. K.; Zhou, H. Y.; Nguyen, S. T.; Torkelson, J. M. Polymer blend compatibilization by gradient copolymer addition during melt processing: Stabilization of dispersed phase to static coarsening. *Macromolecules* **2005**, *38*, 1037–1040.

(42) Kim, J.; Sandoval, R. W.; Dettmer, C. M.; Nguyen, S. T.; Torkelson, J. M. Compatibilized polymer blends with nanoscale or sub-micron dispersed phases achieved by hydrogen-bonding effects: Block copolymer vs blocky gradient copolymer addition. *Polymer* **2008**, *49*, 2686–2697.

(43) Kim, J.; Zhou, H. Y.; Nguyen, S. T.; Torkelson, J. M. Synthesis and application of styrene/4-hydroxystyrene gradient copolymers made by controlled radical polymerization: Compatibilization of immiscible polymer blends via hydrogen-bonding effects. *Polymer* **2006**, *47*, 5799–5809.

(44) Tao, Y.; Kim, J.; Torkelson, J. M. Achievement of quasi-nanostructured polymer blends by solid-state shear pulverization and compatibilization by gradient copolymer addition. *Polymer* **2006**, *47*, 6773–6781.

(45) Wang, R. Phase Behavior of Ternary Homopolymer/Gradient Copolymer Blends. *Macromolecules* **2009**, *42*, 2275–2285.

(46) Carmesin, I.; Kremer, K. The Bond Fluctuation Method - A New Effective Algorithm for the Dynamics of Polymers in All Spatial Dimensions. *Macromolecules* **1988**, *21*, 2819–2823.

(47) Paul, W.; Binder, K.; Heermann, D. W.; Kremer, K. Crossover Scaling in Semidilute Polymer-Solutions - A Monte-Carlo Test. *J. Phys. II* **1991**, *1*, 37–60.

(48) Paul, W.; Binder, K.; Heermann, D. W.; Kremer, K. Dynamics of Polymer-Solutions and Melts - Reptation Predictions and Scaling of Relaxation-Times. *J. Chem. Phys.* **1991**, *95*, 7726–7740.

(49) Baschnagel, J.; Binder, K.; Wittmann, H. P. The Influence of the Cooling Rate on the Glass-Transition and the Glassy State in 3-Dimensional Dense Polymer Melts - a Monte-Carlo Study. *J. Phys.: Condens. Matter* **1993**, *5*, 1597–1618.

(50) Baschnagel, J.; Binder, K. Structural Aspects of a 3-Dimensional Lattice Model for the Glass-Transition of Polymer Melts - a Monte-Carlo Simulation. *Physica A* **1994**, *204*, 47–75.

(51) Binder, K. In *Monte Carlo and Molecular Dynamics Simulations in Polymer Science*; Oxford University Press: New York, 1995; Vol. 17.

(52) Sariban, A.; Binder, K. Spinodal Decomposition of Polymer Mixtures - a Monte-Carlo Simulation. *Macromolecules* **1991**, *24*, 578–592.

(53) Cahn, J. W. Phase Separation by Spinodal Decomposition in Isotropic Systems. *J. Chem. Phys.* **1965**, *42*, 93.

(54) Lifshitz, I. M.; Slyozov, V. V. The Kinetics of Precipitation from Supersaturated Solid Solutions. *J. Phys. Chem. Solids* **1961**, *19*, 35–50.

(55) Siggia, E. D. Late Stages of Spinodal Decomposition in Binary Mixtures. *Phys. Rev. A* **1979**, *20*, 595–605.

(56) Koga, T.; Kawasaki, K. Spinodal Decomposition in Binary Fluids - Effects of Hydrodynamic Interactions. *Phys. Rev. A* **1991**, *44*, R817–R820.

(57) Hashimoto, T.; Takenaka, M.; Jinnai, H. Scattering Studies of Self-Assembling Processes of Polymer Blends in Spinodal Decomposition. *J. Appl. Crystallogr.* **1991**, *24*, 457–466.

(58) Izumitani, T.; Hashimoto, T. Slow Spinodal Decomposition in Binary-Liquid Mixtures of Polymers. *J. Chem. Phys.* **1985**, *83*, 3694–3701.